Preparation, characterisation and *in vitro* antibacterial property of ciprofloxacin-loaded nanostructured lipid carrier for treatment of *Bacillus subtilis* infection

Left Running Head: P. NNAMANI ET AL.

Petra Nnamani [1] * Agatha Ugwu [1] Emmanuel Ibezim [2] Simon Onoja [3] Amelia Odo [4] [AQ2]Maike Windbergs [4] Chiara Rossi [4 5 6][AQ6] Claus-Michael Lehr [1] Anthony Attama [1]

[1]*Department of Pharmaceutics, Faculty of Pharmaceutical Sciences, Drug Delivery and Nanomedicines Research Group, University of Nigeria, Nsukka, Nigeria;*

[2]*Department of Human Nutrition and Dietetics, University of Nigeria, Nsukka, Nigeria;*

[3]*Department of Human Kinetics and Health Education, University of Nigeria, Nsukka, Nigeria;*

[4]*Department of Drug Delivery, Helmholtz Institute for Pharmaceutical Research Saarland (HIPS), Helmholtz Centre for Infection Research, Saarland University, Saarbrücken, Germany;*

[5]*PharmBioTec GmbH, Saarbrücken, Germany;*

[6]*Department of Biopharmaceutics and Pharmaceutical Technology, Saarland University, Saarbrücken, Germany*

**CONTACT Petra Nnamani petra.nnamani@unn.edu.ng; obiomaeze@yahoo.com Department of Pharmaceutics, Faculty of Pharmaceutical Sciences, Drug Delivery and Nanomedicines Research Group, University of Nigeria, Nsukka 410001, Enugu State, Nigeria*

Received: 2018-09-18

Revised: 2019-02-06

Accepted: 2019-02-11

Informa UK Limited, trading as Taylor & Francis Group

ABSTRACT

Objective: Study of controlled ciprofloxacin (CIPRO) nanostructured lipid carriers of Precirol® ATO 5/Transcutol® HP (batch A) and tallow fat/Transcutol® HP (batch B).[AQ3]

Methods: CIPRO concentrations $C_{1–5}$ (0.0, 0.2, 0.5, 0.8, and 1.0% w/w) as $AC_{1–5}$ and $BC_{1–5}$ were prepared by hot homogenisation and characterised by zetasizer, differential scanning calorimetry, Fourier transform infra-red spectroscopy, *in vitro* drug release and growth inhibitory zone diameter (IZD) on agar-seeded *Bacillus subtilis*.

Results: AC_5 achieved polydispersed particles of ~605 nm, 92% encapsulation efficiency (EE) and –28 mV similar to BC_5 (~789 nm, 91% EE, and –31 mV). Crystallinity indices (AC_5 and BC_5) were low at 3 and 5%, respectively. CIPRO release in AC_5 was ~98% in SGF (pH 1.2) and BC_5 similarly ~98% in SIF (pH 6.8).

Conclusions: AC_5 had superior growth inhibition of *B. subtilis* at lower concentration (1.2 µg/mL) than BC_5 and CIPRO controls; hence could serve as possible sustained delivery system of CIPRO.

KEYWORDS Inhibition zone diameter; ciprofloxacin; *Bacillus subtilis*; nanostructured lipid carriers; antimicrobial activity

Introduction

Ciprofloxacin (CIPRO) hydrochloride is a broad spectrum fluoroquinolone antimicrobial agent, frequently used in most Gram positive and Gram negative infections of the urinary tract (complicated and non-complicated), skin and soft tissue, bone and joint, infectious diarrhoea, typhoid fever, chancroid, pneumonia caused by Gram negative bacte-

ria a[illegible]l as acute exacerbation of chronic bronchitis (Egger *et al.* 2001, Charoo *et al.* 2003, Dillen *et al.* 2004, Shah *et al.* 2012). As a fluoroquinolone, its antibacterial action occurs by inhibiting the bacterial topoisomerase II (DNA gyrase) enzyme. Topoisomerases are responsible for continuous introduction of negative supercoils into DNA which is an ATP-dependent reaction that requires both strands of the DNA to be cut to permit passage of a segment of DNA through the break before the break is then resealed. Fluoroquinolone such as CIPRO therefore decreases the introduction of negative supercoils into DNA and causes rapid cessation of DNA synthesis by interfering with the propagation of DNA replication. On the other hand, CIPRO is well absorbed when given orally with a bioavailability of 70% and peak plasma concentration of 1.2 µg/mL achieved after single dose of 250 and 500 mg respectively within 1–2 h of administration (Dillen *et al.* 2004, 2006, Chono *et al.* 2011). Absorption is delayed when CIPRO is given with a meal. CIPRO has wide distribution in the tissues (placenta, lung, skin, fat, muscle, cartilage, bone, and genital tissues) and body fluids (breast milk, saliva, lymph, peritoneal fluid, bile, prostatic and bronchial secretions) as well as partly metabolised in the liver (Chono *et al.* 2011). The plasma half-life is about 3.5–4.5 h but may be prolonged in severe renal insufficiency and in the elderly. The dose of CIPRO varies according to severity of infection but generally employs between 250–500 mg, 500–750 mg, and/or 750–1000 mg every 12 h for 7–14 days. Due to dose frequency (at least twice daily) of these large doses of CIPRO, compliance to long treatment course remains an issue in addition to so many side effects (on gastrointestinal tract, skin, central nervous system, kidney, and blood) and interaction with many possible concomitant drugs (such as analgesics, antacids, antineoplastics, immunosuppressants, etc.) (Chono *et al.* 2011). In other words, non-compliance would imply development of bacterial resistance to this important all-purpose drug which invariably leads to loss of potency.[AQ4]

CIPRO is practically insoluble in water; very slightly soluble in ethanol, methylene chloride and soluble in dilute acetic acid. Its melting point lies between 255 °C and 257 °C with decomposition. Based on today's knowledge, further improvement for a drug such as CIPRO might be possible by its incorporation into an oil-core solid lipid-walled nanoparticle delivery system of nanostructured lipid carriers (NLCs). NLCs have been shown to increase loading capacity hence an improved delivery of actives in addition to higher encapsulation efficiency (EE) due to lesser degree of drug expulsion upon storage (lower crystallinity), protection from degradation in the stomach, controlled release of actives, and above all, low dose regimen with less side effects and improved compliance (Desai *et al.* 2010, Wang *et al.* 2013, Nnamani *et al.* 2014, Pinto *et al.* 2014).[AQ5] Other advantages include low production cost, easy scalability and low toxicity of starting materials since organic solvents are not involved in NLC preparations as well as high versatility of NLC for different routes of administ[illegible]on (Gonzalez-Mira *et al.* 2010, Mitri *et al.* 2011, Gupta *et al.* 2012, Paul *et al.* 2012, 2014, Beloqui *et al.* 2013).

Overall, the present work aims to present NLC formulations of graded concentrations of CIPRO (0.0, 0.2, 0.5, 0.8, and 1.0% w/w) in two different optimised nanocarriers of Precirol® ATO 5/Transcutol® HP (batch A) and tallow fat/Transcutol® HP (batch B) at 3:1 combination respectively to achieve 15% w/w lipid composition. The resultant NLC formulations ($AC_{1–5}$ and $BC_{1–5}$) were characterised and assessed for *in vitro* CIPRO release in bio-relevant media (simulated gastric fluid, SGF, pH 1.2 and simulated intestinal fluid, SIF, pH 6.8) as well as *in vitro* antibacterial growth inhibition of *Bacillus subtilis* on seeded agar plates. *Bacillus subtilis* is a ubiquitous bacterium (Gram-positive and catalase-positive) commonly recovered from water, soil, air, and decomposing plant residue (Edberg 1991). The bacterium produces an endospore that allows it to endure extreme conditions of heat and desiccation in the environment. Given its ubiquity in nature and the environmental conditions under which it is capable of surviving, *B. subtilis* could be expected to temporarily inhabit the skin and gastrointestinal tract of humans, but it is doubtful that this organism would colonise other sites in the human body (Edberg 1991). Though *B. subtilis* is not a frank human pathogen, yet it has on several occasions been isolated from human infections including bacteraemia, endocarditis, pneumonia, and septicaemia especially in patients with compromised immune states followed by inoculation in high numbers of *B. subtilis* (Edberg 1991, Yang *et al.* 2011). There also have been several reported cases of food poisoning attributed to large numbers of *B. subtilis* contaminated food (Edberg 1991, Oggioni *et al.* 1998, El-Feky *et al.* 2009). Even though *B. subtilis* does not produce significant quantities of extracellular enzymes or other factors that would predispose it to cause infection unlike several other species in the genus, still it does produce the extracellular enzyme subtilisin that has been reported to cause allergic or hypersensitivity reactions in individuals repeatedly exposed to it (Edberg 1991, Oggioni *et al.* 1998). Meanwhile, CIPRO has not been listed as first-line treatment for Bacillus infection; instead, antibiotics which appear especially useful in the treatment of Bacillus infections are clindamycin and vancomycin, to which the vast majority of strains are susceptible *in vitro* (Edberg 1991). Unfortunately, these agents

are more costly and less available than CIPRO. Therefore, to investigate the potential of CIPRO-loaded NLCs in inhibiting bacterial growth *in vitro*, *Bacillus subtilis* was seeded in agar plates. The success associated with this investigation would provide basis to make CIPRO also effective against this particular microorganism, by improving its delivery across the ordinarily very hard and impermeable walls of the *B. subtilis* endospore. This envelop surrounding the DNA and other internal cell structures makes them inaccessible to extreme temperatures, chemicals, environmental factors, and even some types of radiation (Oggioni *et al.* 1998, Yang *et al.* 2011). In the light of the above, fewer side effects and possibility to reduce dose and frequency of CIPRO are expected, allowing for better compliance and more effective oral administration.

Materials and methods

Materials

Ciprofloxacin hydrochloride was obtained from Hangzhou Dayang Chem. Co., Ltd. (Hangzhou, China), Polysorbate® 80 (Merck, Darmstadt, Germany), while Precirol® ATO 5 and Transcutol® HP were donated by Gattefossé (Saint-Priest, France). Phospholipon® 90G (P90G) was a gift from Phospholipid GmbH (Cologne, Germany) whereas Poloxamer® 188 and Solutol® HS (BASF, Ludwigshafen, Germany) were received as donations. Tallow fat was obtained from a batch processed in the Department of Pharmaceutics, University of Nigeria Nsukka (UNN). The biorelevant media, SGF (pH 1.2) and SIF (pH 6.8) were prepared without pepsin and pancreatin, respectively. Stock cultures of *Bacillus subtilis were* obtained from the Pharmaceutical Microbiology Unit of Department of Pharmaceutics, UNN. Distilled water was used throughout the study.

Lipid screening

Bulk lipids of tallow fat, Precirol® ATO 5, Phospholipon® 90 G (P90G), Transcutol® HP and their binary mixtures as well as CIPRO were investigated by differential scanning calorimetry (DSC) using a differential scanning calorimeter (NETZSCH DSC 204 FI, Waldkraiburg, Germany). Briefly, lipids were weighed (HH.W21 – Cr42II, Adventurer Ohaus, Shanghai, China), into a crucible and melted together on a hot plate (SR1 UM 52188, Remi Equip., Mumbai, India) at 70 °C and stirred until solidification. Thermal properties were obtained in the range of 35–190 °C at 10 °C/min under a 20 mL/min nitrogen flux with sample sizes of 3–5 mg while using a reference standard of empty aluminium pan. Optimised binary mixtures were obtained at 3:1 combinations of Precirol® ATO 5/Transcutol® HP (batch A) and tallow fat/Transcutol® HP (batch B), respectively.

Production of lipid nanocarriers

All particles were produced by hot homogenisation of optimised matrices of Precirol® ATO 5/Transcutol® HP (batch A) and tallow fat/Transcutol® HP (batch B), each melted at 90 °C and loaded with graded concentration of CIPRO (0, 0.2, 0.5, 0.8, and 1% w/w). To the melted lipid phase, Solutol® HS 15 (5% w/w) and polysorbate 80 (Tween® 80, 2% w/w) were added to enhance CIPRO-solubility whereas Poloxamer® 188 (3% w/w) was added to the aqueous phase and heated to the same temperature before addition to the molten lipid phase. This was followed by high shear homogenisation (Ultra-Turrax, T18 basic, IKA, Staufen, Germany) at 25 000 rpm for 15 min to produce an o/w emulsion which was allowed to cool at room temperature. NLCs containing no drug were also prepared to serve as negative control.

Differential scanning calorimetry

Differential scanning calorimetry was used to analyse the crystallinity of particles using a DSC (NETZSCH DSC 204 FI, Waldkraiburg, Germany) with an empty standard aluminium pan as reference, after baseline correction. Prior to analysis, samples were weighed in aluminium pan to contain solids in the range of 3–5 mg and analysed with a heating rate of 10 °C/min from 35 to 250 °C. During this period, pans were purged by nitrogen gas (20 mL/min) while empty pans served as reference standards. Recrystallisation index (RI %) was calculated using the modified Equation (3) (Freitas and Müller 1999, Keck *et al.* 2014, Nnamani *et al.* 2014).

$$\text{RI}\ (\%) = \frac{\Delta\ H \text{ aqueous lipid nanoparticle dispersion}}{\Delta\ H \text{ bulk material of } P \text{ or } T\ \times\ \text{concentration of solid lipid phase}} \times\ 100 \quad (1)$$

where ΔH aqueous lipid nanoparticle dispersion and ΔH bulk material refer to enthalpies (–mW/mg) of the aqueous lipid nanoparticle (NLC) dispersion and bulk materials of Precirol® ATO 5 and/or tallow fat, respectively. Concentration of solid lipid phase means the actual amount of the solid lipid in the total dispersion (e.g. 15% w/w) dispersion of 3:1 mixture of solid:liquid lipids.

Percentage yield and encapsulation efficiency

Each batch of NLC was weighed after formulation to get the yield while percentage (%) yield was calculated using the formula:

$$\%\ \text{Yield} = \frac{W_1}{W_2 + W_3} \times\ 100 \quad (2)$$

where W_1 is the weight of the NLC formulated (g), W_2 is the weight of the drug added (g), and W_3 is the weight of the lipid matrix and surfactant (g).

Encapsulation efficiency (% EE) of CIPRO in NLCs was determined by UV/VIS spectrophotometry after centrifugation (Heraeus Multifuge® x1R Centrifuge, Yardley, PA) of aliquot sample (5 mL) through centrifugal filter units (Amicon® Ultracel filters, 50 kDa, Darmstadt, Germany) at 2260×*g* at room temperature until at least 1 mL of aqueous phase filtrate was collected. This was used to quantify the amount of non-incorporated CIPRO in aqueous solution by UV-VIS spectrophotometry (6405 Jenway Spectrophotometer, Staffordshire, UK) at λ_{max} of 285.5 nm which was the maximum absorption of CIPRO in aqueous acid (0.1 N HCl). A standard curve of CIPRO in aqueous acid (0.1 N HCl) was used to determine the concentration of CIPRO which was compared with the drug-free NLCs used as control. Considering the amount of CIPRO initially loaded into the NLC formulations and subtracting the free CIPRO remaining in the filtrate, the amount of CIPRO incorporated into the NLCs was determined; hence the % EE was calculated by Equation (2):

$$\%\ EE = \frac{\text{total amount of } CIPRO - \text{free CIPRO in the filtrate}}{\text{total amount of CIPRO}} \times 100 \quad (3)$$

Particle characterisation

Particles were analysed by photon correlation spectroscopy (PCS) using a zetasizer nano-ZS (Malvern Instrument, Worceshire, UK). Samples were diluted with double-distilled water to obtain a suitable scattering intensity, before PCS analysis to obtain size mean diameter (*z*-average, nm), polydispersity index (PDI), and zeta potentials (ZPs, $n = 3$) via electrophoretic mobility measurements while applying the Helmholtz–Smoluchowski equation.

pH-dependent stability of formulations

Time-dependent pH analysis (pHep® Hana Instrument, Padova, Italy) of NLC dispersions were performed post 24 h preparation period and upon room temperature storage at 3 and 6 months respectively for each batch of formulation.

Scanning electron microscopy (SEM)

The morphologies of NLCs (optimised) were determined using SEM measurement (Hitachi S-4000 Microscope, Tarrytown, NY). Samples were diluted with double-distilled water and deposited on film-coated copper grids to air-dry overnight at room temperature. The dried samples were visualised under SEM.

Fourier transform infra-red spectroscopy (FTIR)

The NLC dispersions and pure CIPRO wereas evaluated using Shimadzu FTIR 8300 spectrophotometer (Shimadzu, Tokyo, Japan). All samples were run in triplicates with several controls run in parallels. A background run was performed as a negative control to remove the background noise of the instrument while free CIPRO analysis served as the positive control alongside NLCs. Spectra were recorded in the wavelength region of 4000–400 cm^{-1} with spectral resolution of 4 cm^{-1}.

In vitro release profile and kinetics of release

In vitro drug release studies for the batches of NLCs loaded with CIPRO were studied in 250 mL each of SGF and SIF with the temperature and speed of rotation of each medium maintained at 37 ± 2 °C and 100 rpm, respectively. A quantity of the NLCs containing 100 mg of CIPRO was weighed separately and placed in a polycarbonated dialysis membrane (MWCO 6000–8000, Spectrum Labs, Breda, The Netherlands) which was pre-treated by soaking in distilled water 24 h prior to use. The NLC-containing dialysis membrane was securely tied with a thermo-resistant thread and placed in the appropriate medium. At pre-determined time interval (1–24 h), 5 mL portion of the dissolution medium was withdrawn and absorbance determined at appropriate wavelengths (285.8 and/or 322 nm) in the UV Spectrophotometer (6405 Jenway, Stone, UK). To keep the volume of the dissolution medium constant, 5 mL of fresh medium was added after each withdrawal. The amount of drug released at each time point was calculated with reference to the relevant Beer's plot.

The kinetics and mechanisms of CIPRO release from formulations were studied using different release models (zero order, first order, Higuchi, and Ritger–Peppas) according to standard protocols to describe Higuchi release model (cumulative % drug release versus square root of time), first order (log cumulative of percentage drug remaining versus time), zero order (cumulative percentage drug release versus tin) and Ritger–Peppas (Fickian and/or non-Fickian release through Log ($Mt/M\infty$) = Log k + n Log t) (Nnamani *et al.* 3, Agubata *et al.* 2015).

Release as a function of inhibition zone diameter

The plate agar diffusion method was used for this study conducted after 1 month of NLC formulation (Attama *et al.* 2009, Nnamani *et al.*). Briefly, three loopfuls of *Bacillus subtilis* was introduced into different sterile Petri dishes, to which 20 mL of sterile molten nutrient agar was poured separately, swirled gently and allowed to solidify. A sterile cork borer was used to bore holes on the solidified sterile agar plates. Different concentrations of pure sample of CIPRO and unknown concentration of the formulated NLC-loaded CIPRO were introduced into the corresponding holes and/or cups. The plates were allowed a pre-diffusion period of 30 min upon standing before incubation at 37 °C for 24 h. The resultant growth IZD of each hole was measured and recorded. The procedure was repeated using a commercial brand of CIPRO (Ciprotab®), as control. The concentration of the formulated NLC-loaded CIPRO was determined by the graphical method (Attama *et al.* 2009, Nnamani *et al.*).

Statistical analysis

Results were expressed as mean ± standard deviation. One-way ANOVA was used to assess the difference between groups while Microsoft Excel and STATA II software packages were used for all analyses. Statistical significance was determined using Student's t-test, with $p < 0.05$ considered to be statistically significant.

Results

Lipid screening and thermal properties of formulations

Bulk materials of tallow fat and Precirol® ATO 5 as well as optimised binary matrices (3:1) of Precirol® ATO 5/ Transcutol® HP (batch A) and Tallow fat/Transcutol® HP (batch B) are shown in Figure 1. Selection was based on lower values of enthalpy as an index of low crystallinity. Thermal properties of formulations are shown in Table 1.

Figure 1. DSC thermograms of lipid matrices. (A) Tallow fat (m. pt 56.4 °C and enthalpy 27.84 -mW/mg), (B) Precirol® ATO 5 (m. pt 71 °C and enthalpy 37.59 -mW/mg), (C) Tallow fat + Transcutol® HP matrix (m. pt 56.5 °C and enthalpy 9.5 -mW/mg), (D) Precirol® ATO 5 + Transcutol® HP (m. pt 143.7 °C and enthalpy 5.6 -mW/mg). Less crystalline matrices have low enthalpy values (selected from Table 1).

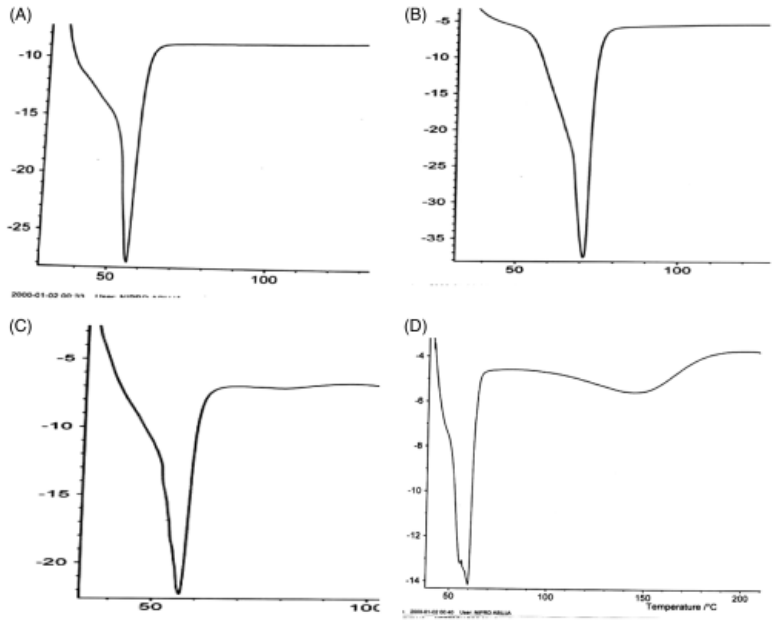

Table 1. Thermal properties of formulations and bulk materials.Table Layout

Lipid matrix	Melting peak (°C)	Enthalpy (–mW/mg)	Onset melting point (°C)	Enthalpy (–mW/mg)	Recrystallisation index (%)
CIPRO	155.6	7.17	255	7.17	–
AC1 (blank formulation)	134.6	10.92		–	3.49
AC2	248.2	17.54	95.5	–	3.48
AC3	59.7	14.15	–	–	4.52
AC4	60.3	20.27	–	–	6.47
AC5	145.2	22.31	56.5	9.48	3.03
BC1 (blank formulation)	56.2	42.56	–	–	10.06
BC2	57.5	24.95	–	–	5.90
BC3	55.5	23.87	–	–	5.64
BC4	61.2	32.40	–	–	7.66
BC5	53.4	21.80	–	–	5.16
Precirol® ATO 5	71.0	37.59	–	–	–
Tallow fat	56.4	27.84	–	–	–
Transcutol® HP	164.4	26.76	130.3	13.63	–
Precirol + Transcutol® HP (3:1)	143.7	14.15	59.7	5.551	–

Screening of (A) single entity lipids (Precirol® ATO 5, Tallow fat, Transcutol® HP and P90G®) and drug (CIPRO); (B) mixtures (binary lipids: tallow fat + P90G® and Precirol + P90G®); (nanostructured lipids: tallow fat + Transcutol® HP and Precirol + Transcutol® HP). Mixtures were obtained at different ratios of 1:1, 1:2, and 1:3 ratios (data not shown). Low crystallinity of matrices based on enthalpy values was used as criteria for selection ($N = 3$). Nanostructured lipid of Tallow fat + Transcutol® HP and Precirol + Transcutol® HP were less crystalline than binary mixtures of tallow fat + P90G® and Precirol + P90G®.

Lipid matrix	Melting peak (°C)	Enthalpy (–mW/mg)	Onset melting point (°C)	Enthalpy (–mW/mg)	Recrystallisation index (%)
Tallow fat + Transcutol® HP (3:1)	56.5	22.31	56.5	9.483	–
P90G®	280.9	25.98	130.8	13.13	–
Precirol + P90G®	60.3	20.27	–	–	–
Tallow fat + P90G®	57.5	28.00	–	–	–
Screening of (A) single entity lipids (Precirol® ATO 5, Tallow fat, Transcutol® HP and P90G®) and drug (CIPRO); (B) mixtures (binary lipids: tallow fat + P90G® and Precirol + P90G®); (nanostructured lipids: tallow fat + Transcutol® HP and Precirol + Transcutol® HP). Mixtures were obtained at different ratios of 1:1, 1:2, and 1:3 ratios (data not shown). Low crystallinity of matrices based on enthalpy values was used as criteria for selection ($N = 3$). Nanostructured lipid of Tallow fat + Transcutol® HP and Precirol + Transcutol® HP were less crystalline than binary mixtures of tallow fat + P90G® and Precirol + P90G®.					

Particle characterisation

Table 2 shows general particle properties of NLCs. It could be seen that the particle size for batches of $AC_{1–5}$ was smaller (~320–903 nm) than those of $BC_{1–5}$ (~789 nm–3158 µm), even though both batches were polydispersed with PDI above 0.25. Besides, the NLC particles were very stable (about –30 mV) even upon storage at room temperature for over 6 months despite slight fluctuations in the pH of the dispersion. The particles also generally had high yield (%) and % EE. The pH stability results of all NLC formulations generally showed all samples post 24 h preparation as having higher pH values than upon storage for 3 and 6 months.

Table 2. Particle characterisation.Table Layout

Batches	Zeta potential (mV) ± SD	Polydispersity index (PdI) ± SD	*Z*-Ave (nm) ± SD	Encapsulation efficiency (% v/v) ± SD	Yield (%) ± SD
AC1 (Blank)	−29.0 ± 0.28	0.52 ± 0.39	903.2 ± 27.22*	–	44.1* ± 0.01
AC2	−27.8 ± 0.21	0.49 ± 0.25	319.2 ± 5.09	81.4 ± 0.11	58.4 ± 0.20
AC3	−27.1 ± 0.11	0.46 ± 0.28	825.9 ± 17.05	75.2 ± 0.13	60.8 ± 0.12
AC4	−27.0 ± 0.18	0.40 ± 0.22	437.9 ± 9.91	89.4 ± 0.21	86.2 ± 0.23
AC5	−28.2** ± 0.01	0.42 ± 0.32	604.7 ± 12.06**	92.4** ± 0.31	85.7** ± 0.24
BC1 (Blank)	−34.8 ± 0.31	0.68 ± 0.54	927.2 ± 25.24*	–	35.3* ± 0.19
BC2	−18.9 ± 0.27	0.85 ± 0.79	3158 ± 32.33	77.8 ± 0.12	43.9 ± 0.17
BC3	−30.2 ± 0.09	0.81 ± 0.73	1428 ± 30.41	81.5 ± 0.13	81.2 ± 0.24
BC4	−28.2 ± 0.15	0.88 ± 0.82	1672 ± 28.73	82.4 ± 0.15	83.3 ± 0.15
BC5	−30.5** ± 0.01	0.67 ± 0.43	788.7 ± 14.22**	90.8** ± 0.21	86.2** ± 0.11
SD: standard deviation.					
Optimised formulations (AC5** and BC5**) reflect outstanding performance of the CIPRO batches compared to blank formulations AC1* and BC1* ($p < 0.05$). $n = 3$.					

Microscopy

SEM measurement was used to study morphology of NLC optimised formulations (Figure 2). It could be seen that the CIPRO-loaded NLCs of AC_5 and BC_5 as well as blank NLCs (AC_1 and BC_1) appeared spherical and/or elliptical (Nnamani *et al.* 2014).

Figure 2. SEM images (AC_5) Optimized CIPRO-NLC from Precirol® ATO_5 + Transcutol® HP; (BC_5) Optimized CIPRO-NLC from Tallow fat + Transcutol® HP; (AC_1) Blank formulation of Precirol® ATO_5 + Transcutol® HP; (BC_1) Blank formulation of Tallow fat + Transcutol® HP.

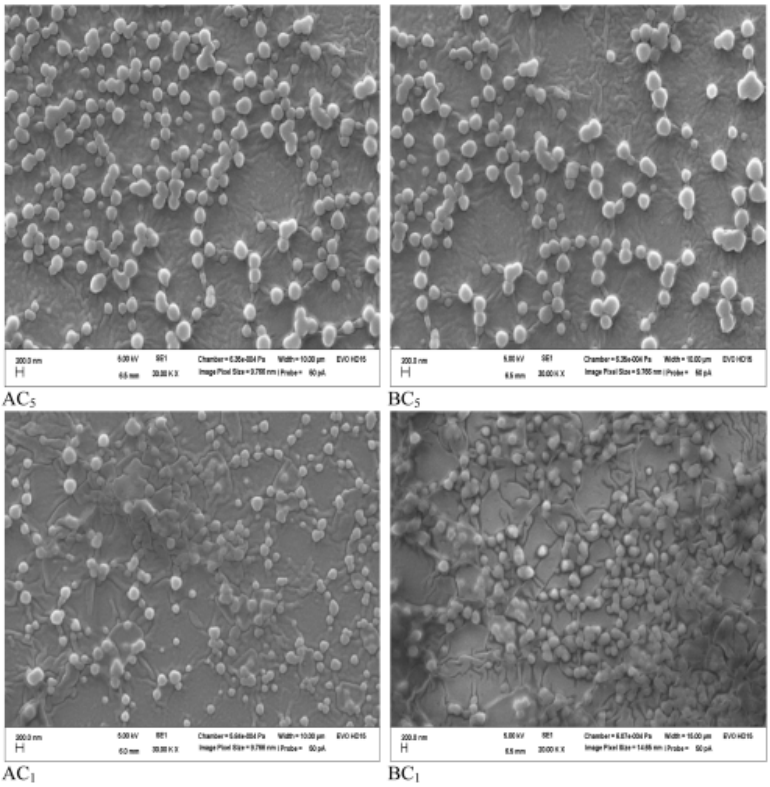

FTIR

To demonstrate the possibility of incorporation of CIPRO into NLC, IR spectra of NLC matrices, CIPRO-loaded NLCs (AC_5 and BC_5), and bulk entity of CIPRO were obtained and presented in Figure 3.

Figure 3. FTIR spectra. TT means Tallow fat/Transcutol® HP; PT means Precirol® ATO_5 and Transcutol® HP; BC® implies optimized CIPRO formulation from TT batch; AC_5 implies optimized CIPRO formulation from PT batch..

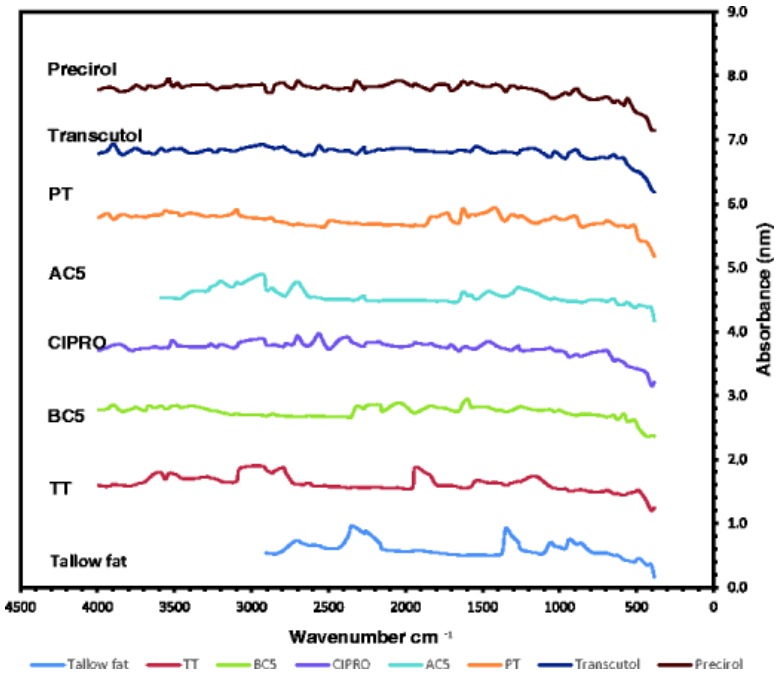

In vitro drug release and mechanism of kinetics

The *in vitro* release profile of optimised NLCs was determined in SGF (pH 1.2) and SIF (pH 6.8) and shown in Figure 4. Within the first 10 h of release study, only CIPRO amount (<30%) was released across all samples and media despite inclusion of both water-soluble (Poloxamer® 188) and oil-soluble surfactants (Solutol® HS and Polysorbate 80) which ordinarily could increase porosity of the matrix for easier fluid penetration and release (Agubata *et al.* 2015). Overall, the kinetics of CIPRO release from NLCs showed that Higuchi was the predominant mechanism of release (Table 3) having recorded the highest R^2 values generally in all media despite having very slow release of CIPRO (<30%) in 10 h of release study. This was not surprising considering the high EE (%) of CIPRO in the low crystalline NLCs which could make it inaccessible immediately for release until much later (post 20 h).

Figure 4. (A) *In vitro* release profile of ciprofloxacin in SGF ($n = 3$) and (B) *in vitro* release profile of ciprofloxacin in SIF ($n = 3$).

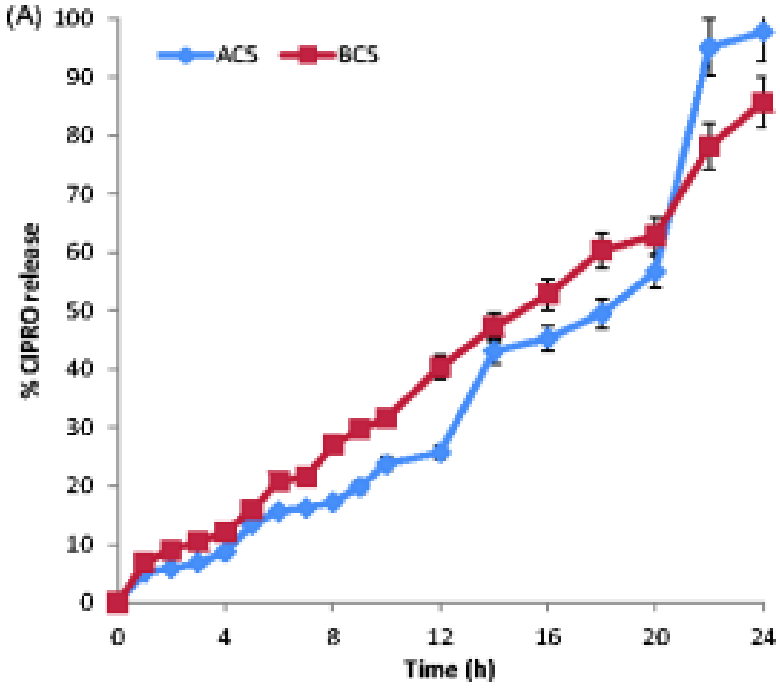
(A)
ACS
BCS
% CIPRO release
Time (h)
0
10
20
30
40
50
60
70
80
90
100
0
4
8
12
16
20
24

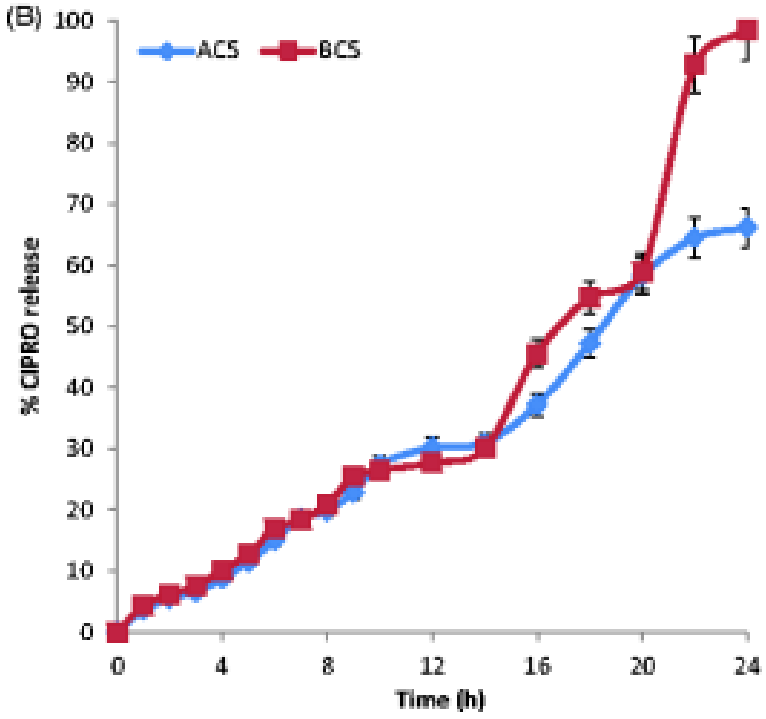
(B)
ACS
BCS
% CIPRO release
Time (h)
0
10
20
30
40
50
60
70
80
90
100
0
4
8
12
16
20
24

Table 3. Kinetics of CIPRO release from NLC.Table Layout

Drug	Media	Batches	Zero order (R^2)	First order (R^2)	Higuchi (R^2)	Ritger–Peppas parameters	
						R^2	N
CIPRO	SGF	AC_5	0.903	0.626	0.919	0.920	1.002
		BC_5	0.990	0.895	0.963	0.840	0.359
	SIF	AC_5	0.909	0.936	0.951	0.980	1.001
		BC_5	0.979	0.6129	0.975	0.956	1.01
Release was predominantly Higuchi model, based on porosity of matrices, followed by the Peppas model.							

Release study as a function of inhibition zone diameter

Post 24 h incubation of the *B. subtilis* seeded agar plates with CIPRO-loaded NLCs, our observations showed that AC_5 recorded the overall highest (mean) IZD (24 mm) on *B. subtilis* at much lower concentration (1.2 µg/mL) than the pure drug (7.5 µg/mL) and/or commercial sample (7.5 µg/mL), which had IZDs of 22 mm respectively, as shown in Figure 5. Comparatively AC_5 recorded higher IZD (24 mm) than BC_5 (18 mm) even at equal concentration (2.2 µg/mL).

Figure 5. (A) IZD (mm) of pure CIPRO sample and optimised NLCs (AC5 and BC5) and (B) IZD (mm) of commercial CIPRO sample and optimised NLCs (AC5 and BC5).

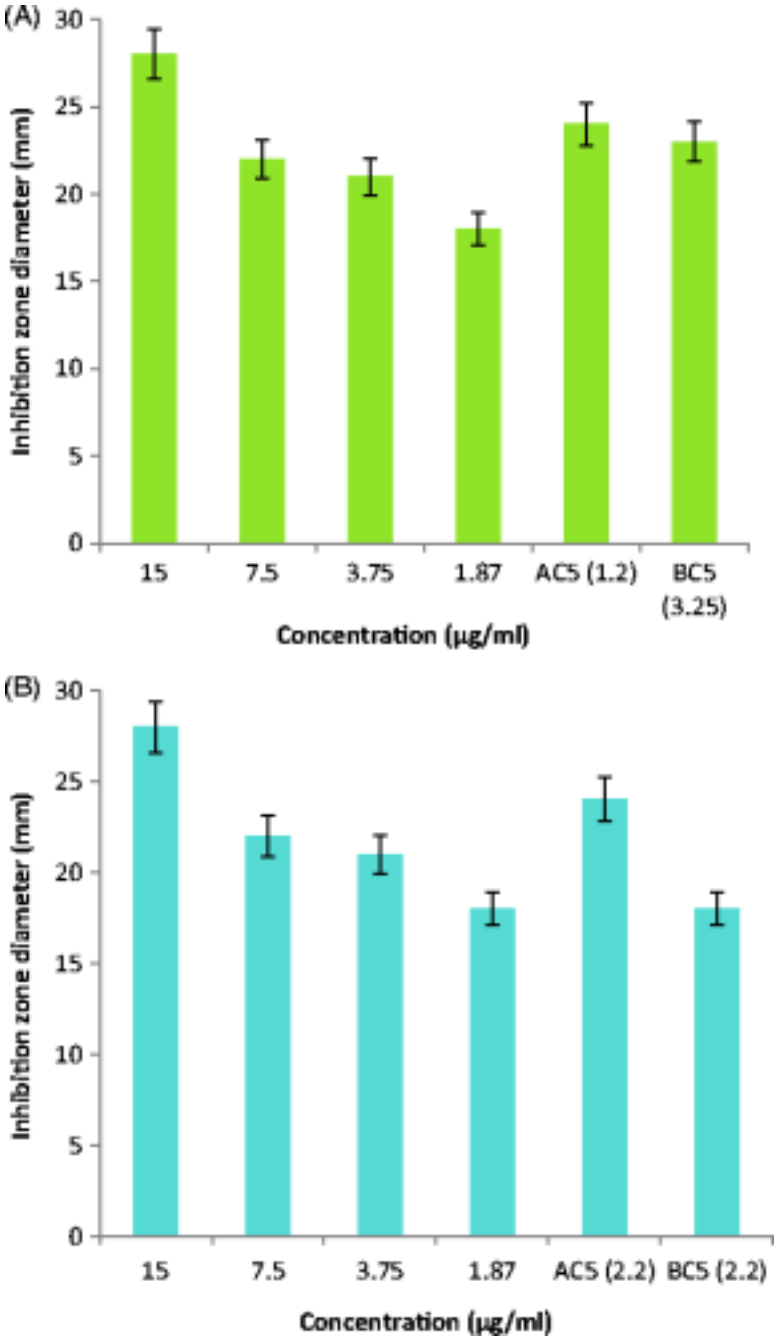

Discussion

The crystallinity of the NLCs could be confirmed using DSC by comparing the melting enthalpy of bulk materials with those of NLC which were much smaller. While the bulk lipids contained 100% of solid lipids of Precirol® ATO 5 and/or tallow fat, the NLCs only consisted of 15% of the lipid mixture at 3:1 of solid lipid (11.25 g) and liquid lipid (3.75 g), respectively. NLC batch A produced from Precirol® ATO 5/Transcutol® HP was named AC_{1-5} whereas batch B corresponding to Tallow fat/Transcutol® HP was termed BC_{1-5} to describe the CIPRO-graded concentrations of 0, 0.2, 0.5, 0.8, and 1% w/w in each batch. Matrix crystallinity was independent of CIPRO concentration. In order

words, AC_5 and BC_5 each containing 1% w/w concentration of CIPRO in each batch of NLC had the least enthalpy values of –9.48 and –21.8 mW/mg respectively when compared to other formulations. To better estimate the degree of crystallinity, the RI was ascertained at 3 and 5% for both AC_5 and BC_5, as the least among their respective batches of formulation. This suggests that despite low crystallinity of NLCs, there was still slight degree of crystallinity remaining which could rightly describe the definition of lipid nanoparticles as being solid at body temperature (Müller *et al.* 2011). Besides, decreased crystallinity corresponded to lower particle sizes (Puglia *et al.* 2013, Keck *et al.* 2014). Zeta potential predicts physical stability of dispersions and the higher the value (positive or negative) the better the stability to avoid aggregation of particles. Since the particles existed in the neighbourhood of –30 mV, they could be said to be stable. Overall in batch A, AC_5 had the highest yield (85.7%) and EE (92.4%) whereas in batch B, BC_5 similarly had 86.2% Y and 90.8% EE. This agreed with the thermal properties of AC_5 and BC_5 with least values of enthalpy (–9.48 and –21.8 mW/mg) and recrystallisation indices of 3% and 5%, respectively, confirming their propensity for higher drug payload without expulsion even upon storage; hence the high ZP (–28 and –30.3 mV) values which also could attest to stability of the systems.

$AC_{1–5}$ samples had pH in the range of 4.2–6.1 whereas those of $BC_{1–5}$ had 3.2–5.4. However, there were slight changes in pH upon storage but this trend was worse in the $BC_{1–5}$ samples. The AC_5 and BC_5 were most stable upon storage in agreement with other observations from particle characterisation and thermal analysis. It could therefore be said that AC_5 and BC_5 be regarded as the optimised samples for further evaluations and that entrapment of CIPRO into the NLC particles did not affect their morphology as well. There was nanoparticle aggregation in the blank formulation shown in Figure 2 (AC1 and BC1) whereas optimised formulations of AC5 and BC5 generally showed polydispersed spherical particles. The shape of solid lipid nanocarriers has been reported to be dependent on the purity of the lipids used (Nnamani *et al.* 2014) and particles prepared using chemically polydispersed lipids are typically spherical (Nnamani *et al.* 2014). The lipid matrix used consisted of a mixture of solid lipids (Precirol® ATO 5 and Tallow fat) and liquid lipid (Transcutol® HP), which suggests that the lipid matrix was chemically polydispersed as well as highly pure.

The interaction study (Figure 3) showed principal peaks at wave numbers 2800–3000, 2220–2255, 1703–1619, and 1267 cm^{-1} (KBr pellets) as due to the vibration of functional groups (C–H, C≡N, C–O, and CC acyclic, aliphatic chain vibration) present in the structure of CIPRO which could also be seen in the FT-IR spectra of the crystalline CIPRO and NLC matrices (PT and TT). Spectra of blank NLCs without CIPRO did not show these peaks, indicating successful incorporation of drug into the CIPRO-containing NLC formulations.

The poor initial release of CIPRO (Figure 4) from the oily-core of the NLC lipid matrix could perhaps be due to efficient encapsulation (Üner and Yener 2007). This is supported by the fact that as time progressed, release became more consistent and post 20 h, there was fast release of CIPRO attesting to its efficient localisation in the oily-core of the particles. This raises hope in actualising a regimen that can comfortably be administered once daily, to improve compliance over conventional twice-daily tablets. Meanwhile, without any dose dumping, CIPRO release was gradually prolonged to 24 h achieving same percentage release of ~98% for AC_5 in SGF and BC_5 in SIF, respectively. On the other note, BC_5 released ~86% of CIPRO in SGF and 66% from AC_5 in SIF respectively too. The two formulations therefore suggest that excipient choice influences performance of formulations thereof. This implies that AC_5 with ~98% CIPRO-release in SGF can be targeted in the gastric area and BC_5 similarly can be targeted in intestinal area.

Release in this study predominantly (Table 3) depended on the porosity of the NLC matrix enclosing CIPRO, as explained by the Higuchi model which deals with release from porous systems (Koga *et al.* 2006, Agubata *et al.* 2015); followed by Zero order. Meanwhile, Peppas mechanism of CIPRO release could be described by release exponent 'n' value and kinetic constant 'k' which incorporates the structural and geometric characteristics of the release device (NLC). Therefore, since the n values were generally greater than 0.45 and 0.81 (though 0.35 for BC_5 in SGF), Fickian diffusion predominated, whereas others with *n* values of 1 followed super case II transport (matrix erosion) and non-Fickian diffusion (Rama Prasad *et al.* 2003).

In vitro growth inhibition study showed that AC_5 released enough CIPRO that diffused out of the NLC matrix to penetrate the endospore surrounding the DNA and other internal cell structures of *B. subtilis* bacteria within 24 h of incubation (Figure 5), thereby decreasing the introduction of negative supercoils into DNA; hence rapid cessation of

DNA synthesis through interference with the propagation of DNA replication. Additionally, the presence of surfactants both hydrophilic and lipophilic could have aided fluidisation of the cell membrane of this organism thereby facilitating penetration of the drug (Krugliak *et al.* 1995, Rama Prasad *et al.* 2003, Koga *et al.* 2006). These observations agree with literature and could probably have aided growth inhibition of *B. subtilis* ($AC_5 > BC_5$) even in lower CIPRO concentration compared to those of pure drug and/or commercial sample (Krugliak *et al.* 1995, Baek and An 2011, Kim and An 2012, Hsueh *et al.* 2015). This was rather not surprising from the point of view of the high drug EE of 92%, *in vitro* drug release in bio-relevant media (~98%) and high negative values of ZP (–28.2 to –30) which could predict good permeation through the cell wall of the film-forming bacteria (Krugliak *et al.* 1995, Rama Prasad *et al.* 2003, Pinto *et al.* 2014).

Conclusions

CIPRO-NLC formulation is acceptable alternative that can reduce the disadvantages of CIPRO-powder/capsule and/or tablets such as frequent dosing of large doses, long treatment courses (7–14 days), non-compliance and development of resistance. CIPRO-NLCs prepared using two solid fats (Precirol® ATO 5 and Tallow fat) and a liquid lipid (Transcutol® HP) produced nanoparticles with acceptable properties. Lower doses of AC5 (1.2 µg/mL) showed better *in vitro* growth inhibition of *B. subtilis* than BC5 (3.25 µg/mL) and pure CIPRO powder and/or commercial tablet (7.5 µg/mL). CIPRO-NLC formulations are efficient carriers for oral delivery of CIPRO, with targeted uptake through the lymphatics. This avoids wide distribution (in tissues, body fluids and the liver) associated with conventional marketed CIPRO-tablet forms. In an outlook for further studies, safety tests and cell penetration studies will prove this concept.

Acknowledgements

We appreciate the assistance of Mr. Kalu Ogboso for antimicrobial studies and Dr. Chiara Rossi for SEM analysis. We thank Phospholipid GmbH Köln, Germany, BASF Ludwigshafen, Germany and Gattefossé, St. Priest, France for gift samples of Phospholipon® 90G; Poloxamer® 188 and Solutol® HS 15; and Precirol® ATO 5 and Transcutol® HP, respectively.

Disclosure statement

No potential conflict of interest was reported by the authors.

ORCID

Petra Nnamani

Claus-Michael Lehr

References

Agubata, C.O., *et al.*, 2015. Formulation, characterization and anti-malarial activity of homolipid-based[AQ7] artemether microparticles. *International journal of pharmaceutics*, **478** (1), 202–222.

Attama, A.A., *et al.*, 2009. Formulation and *in vitro* evaluation of a PEGylated microscopic lipospheres delivery system for ceftriaxone sodium. *Drug delivery*, **16** (8), 448–616.

Baek, Y.W. and An, Y.J., 2011. Microbial toxicity of metal oxide nanoparticles (CuO, NiO, ZnO and Sb_2O_3) to *Escherichia coli*, *Bacillus subtilis* and *streptococcus aureus*. *Science of the total environment*, **409** (8), 1603–1608.

Beloqui, A., *et al.*, 2013. Biodistribution of nanostructured lipid carriers (NLCs) after intravenous administration to rats: influence of technological factors. *European journal of pharmaceutics and biopharmaceutics*, **84** (2), 309–314.

Charoo, N.A., *et al.*, 2003. Ophthalmic delivery of ciprofloxacin hydrochloride from different polymer formulations: *in vitro* and *in vivo* studies. *Drug development and industrial pharmacy*, **29** (2), 215–221.

Chono, S., *et al.*, 2011. Efficient drug delivery to lung epithelial lining fluid by aerosolization of ciprofloxacin incorporated into PEGylated liposomes for treatment of respiratory infections. *Drug development and industrial pharmacy*, **37** (4), 367–372.

Desai, P., Patlolla, R.R., and Singh, M.R., 2010. Interaction of nanoparticles and cell-penetrating peptides with skin for transdermal drug delivery. *Molecular membrane biology*, **27** (7), 247–259.

Dillen, K., *et al.*, 2004. Factorial design, physicochemical characterisation and activity of ciprofloxacin-PLGA nanoparticles. *International journal of pharmaceutics*, **275** (1–2), 171–187.

Dillen, K., *et al.*, 2006. Evaluation of ciprofloxacin-loaded Eudragit RS100 or RL100/PLGA nanoparticles. *International journal of pharmaceutics*, **314** (1), 72–82.

Edberg, S. C., 1991. US EPA human health assessment: Bacillus subtilis. Unpublished. U.S. Environmental Protection Agency, Washington, DC.

Egger, S.F., *et al.*, 2001. *In vitro* susceptibilities to topical antibiotics of bacteria isolated from the surface of clinically symptomatic eyes. *Ophthalmic research*, **33** (2), 117–120.

El-Feky, M.A., *et al.*, 2009. Effect of ciprofloxacin and N-acetylcysteine on bacterial adherence and biofilm formation on ureteral stent surfaces. *Polish journal of microbiology*, **58** (3), 261–267.

Fang, C.-L., Al-Suwayeh, S.A., and Fang, J.-Y., 2013. Nanostructured lipid carriers (NLCs) for drug delivery and targeting. *Recent patents on nanotechnology*, **7** (1), 41–55.

Freitas, C. and Müller, R.H., 1999. Correlation between long-term stability of solid lipid nanoparticles (SLN) and crystallinity of the lipid phase. *European journal of pharmaceutics and biopharmaceutics*, **47** (2), 125–132.

Gonzalez-Mira, E., *et al.*, 2010. Design and ocular tolerance of flurbiprofen loaded ultrasound-engineered NLC. *Colloids and surfaces B*, **81** (2), 412–421.

Gupta, M., Agrawal, U., and Vyas, S.P., 2012. Nanocarrier-based topical drug delivery for the treatment of skin diseases. *Expert opinion on drug delivery*, **9** (7), 783–804.

Hsueh, Y.H., *et al.*, 2015. ZnO nanoparticles affect *Bacillus subtilis* cell growth and biofilm formation. *PLoS one*, **10** (6), e0128457.

Keck, C.M., *et al.*, 2014. Oil-enriched, ultra-small nanostructured lipid carriers (usNLC): a novel delivery system based on flip-flop structure. *International journal of pharmaceutics*, **477** (1–2), 227–235.

Kim, S.W. and An, Y.J., 2012. Effect of ZnO and TiO_2 nanoparticles preilluminated with UVA and UVB light on *Escherichia coli* and *Bacillus subtilis*. *Applied microbiology and biotechnology*, **95** (1), 243–253.

Koga, K., *et al.*, 2006. Enhancing mechanism of Labrasol on intestinal membrane permeability of the hydrophilic drug gentamicin sulfate. *European journal of pharmaceutics and biopharmaceutics*, **64** (1), 82–91.

Krugliak, M., *et al.*, 1995. Antimalarial effects of C18 fatty acids on *Plasmodium falciparum* in culture and on *Plasmodium vinckei petteri* and *Plasmodium yoelii nigeriensis in vivo*. *Experimental parasitology*, **81** (1), 97–105.

Mitri, K., *et al.*, 2011. Lipid nanocarriers for dermal delivery of lutein: preparation characterization, stability and performance. *International journal of pharmaceutics*, **414** (1–2), 267–275.

Müller, R.H., Shegokar, R., and Keck, C.M., 2011. 20 years of lipid nanoparticles (SLN and NLC): present state of development and industrial applications. *Current drug discovery technologies*, **8**, 207–227.

Nnamani, P.O., *et al.*, 2013. Pharmacodynamics of Piroxicam from novel solid lipid microparticles formulated with homolipids from *Bos indicus*. *Current drug delivery*, **10** (6), 645–655.

Nnamani, P.O., *et al.*, 2013. Transdermal microgels of gentamicin. *European journal of pharmaceutics and biopharmaceutics*, **84** (2), 345–354.

Nnamani, P.O., *et al.*, 2014. Development of artemether-loaded nanostructured lipid carrier (NLC) formulation for topical application. *International journal of pharmaceutics*, **477** (1–2), 208–217.

Oggioni, M.R., *et al.*, 1998. Recurrent septicemia in an immunocompromised patient due to probiotic strains of *Bacillus subtilis*. *Journal of clinical microbiology*, **36**, 325–326.

Paul, C., *et al.*, 2012. Evidence-based recommendations on topical treatment and phototherapy of psoriasis: systematic review and expert opinion of a panel of dermatologists. *Journal of the European academy of dermatology and venereology*, **26**, 1–10.

Paul, C., *et al.*, 2014. A new topical formulation for psoriasis: development of methotrexate-loaded nanostructured lipid carriers. *International journal of pharmaceutics*, **477**, 519–526.

Puglia, C., *et al.*, 2013. Optimization of curcumin loaded lipid nanoparticles formulated using high shear homogenization (HSH) and ultrasonication (US) methods. *Journal of nanoscience and nanotechnology*, **13** (10), 6888–6893.

Rama Prasad, Y.V., *et al.*, 2003. Evaluation of oral formulations of gentamicin containing Labrasol in beagle dogs. *International journal of pharmaceutics*, **268** (1–2), 13–21.

Shah, M. and Agrawal, Y., 2012. Ciprofloxacin hydrochloride-loaded glyceryl monostearate nanoparticle: factorial design of Lutrol F68 and Phospholipon 90G. *Journal of microencapsulation*, **29** (4), 331–343.

Shah, M., *et al.*, 2012. Solid lipid nanoparticles of water soluble drug, ciprofloxacin hydrochloride. *Indian journal of pharmaceutical sciences*, **74** (5), 434–442.

Üner, M. and Yener, G., 2007. Importance of solid lipid nanoparticles (SLN) in various administration routes and future perspectives. *International journal of nanomedicine*, **2**, 289–300.

Yang, Y., *et al.*, 2011. Mannitol-guided delivery of ciprofloxacin in artificial cystic fibrosis mucus model. *Biotechnology and bioengineering*, **108** (6), 1441–1449.

Author Queries

Query: AQ1: Please review the table of contributors below and confirm that the first and last names are structured correctly and that the authors are listed in the correct order of contribution. This check is to ensure that your names will appear correctly online and when the article is indexed.

Sequence	Prefix	Given name(s)	Surname	Suffix
1		Petra	Nnamani	
2		Agatha	Ugwu	
3		Emmanuel	Ibezim	
4		Simon	Onoja	
5		Amelia	Odo	
6		Maike	Windbergs	
7		Chiara	Rossi	
8		Claus-Michael	Lehr	
9		Anthony	Attama	

Response: Resolved

Query: AQ2: Please check author names have been typeset correctly and correct if inaccurate.
Response: Petra Nnamani 1, 4; Agatha Ugwu 1; Emmanuel Ibezim 1; Simon Onoja 2; Amelia Odo 3; Maike Windberg 4; Chiara Rossi 4; Claus-Michael Lehr 4, 5; Anthony Attama 1

Query: AQ3: Please modify your present abstract using the headings “context, objective, materials and methods, results, discussion and conclusion”, as per journal style.
Response: Context: In this study, controlled ciprofloxacin (CIPRO) nanostrustructured lipid carriers of Precirol® ATO 5/Transcutol® HP (batch A) and tallow fat/Transcutol® HP (batch B) was carreid out. Objective: The aim was to improve solubility and bioavailability of CIPRO.

Query: AQ4: Please modify your present body of the article using the headings “introduction; methods; results; discussion; conclusions”, as per journal style.
Response: The introduction, methods, results, discussion and conclusion sessions are acceptable to me.

Query: AQ5: The reference (Pinto et al. 2014) is cited in the text but is not listed in the references list. Please either delete the in-text citation or provide full reference details following journal style.
Response: Pinto MF, Moura CC, Nunes C, Segundo MA, Costa Lima SA, Reis S. A new topical formulation for psoriasis: Development of methotrexate-loaded nanostructured lipid carriers. Int Pharm 477 (2014) 519–526

Query: AQ6: The ORCID details of the authors have been validated against ORCID registry. please check the ORCID ID details of the authors.
Response: Maike Windbergs4; Chiara Rossi4Claus-Michael Lehr 4,5 (Please cancel 6).4Department of Drug Delivery, Helmholtz Institute for Pharmaceutical Research Saarland (HIPS), Saarland University, Saarbrücken, Germany5Helmholtz Centre for Infection Research (HZI), Saarland University, Saarbrücken, Germany

Query: AQ7: The references (Fang et al 2013, Nnamani et al 2013, Paul et al 2014, Shah et al 2012) reference list provided but citation is not found in the text
Response: All missing references have been fixed at their respective locations in text.

Comments

C1 Author: Nnamani et al., 2013a Nnamani, P.O., et al., 2013a. Pharmacodynamics of Piroxicam from Novel Solid Lipid Microparticles Formulated with Homolipids from Bos indicus Curr Drug Deliv, 10 (6), 645-655.; :
C2 Author: Nnamani et al., 2013b.... (the two Nnamani et al., 2013 under this section) Nnamani, P.O., et al., 2013b. Transdermal microgels of gentamicin. Eur J Pharm Biopharm, 84, 345-354.; :

C3 Author: Nnamani et al., 2013b; :
C4 Author: Shah et al., 2012a, Shah et al., 2012b; :
C5 Author: Fang et al., 2013; :